available at www.sciencedirect.com
journal homepage: www.europeanurology.com

European Association of Urology

Platinum Priority – Prostate Cancer – Editor's Choice

Editorial by Frédéric Pouliot, Louise Emmett on pp. 371–372 of this issue

Diagnostic Performance and Safety of Positron Emission Tomography with ^{18}F-rhPSMA-7.3 in Patients with Newly Diagnosed Unfavourable Intermediate- to Very-high-risk Prostate Cancer: Results from a Phase 3, Prospective, Multicentre Study (LIGHTHOUSE)

Devaki Shilpa Surasi [a,], Matthias Eiber [b], Tobias Maurer [c,d], Mark A. Preston [e], Brian T. Helfand [f], David Josephson [g,h], Ashutosh K. Tewari [i], Diederik M. Somford [j,k], Soroush Rais-Bahrami [l], Bridget F. Koontz [m,†], Peter J. Bostrom [n,o], Albert Chau [p], Phillip Davis [q], David M. Schuster [r], Brian F. Chapin [s], on behalf of the LIGHTHOUSE Study Group [1]*

[a] *Department of Nuclear Medicine, The University of Texas MD Anderson Cancer Center, Houston, TX, USA;* [b] *Department of Nuclear Medicine, Klinikum rechts der Isar, Technische Universität München, Munich, Germany;* [c] *Martini-Klinik, Hamburg, Germany;* [d] *Department of Urology, University Hospital Hamburg-Eppendorf, Hamburg, Germany;* [e] *Brigham and Women's Hospital, Boston, MA, USA;* [f] *NorthShore University HealthSystem, Evanston, IL, USA;* [g] *Tower Urology, Los Angeles, CA, USA;* [h] *Cedars Sinai Medical Center, Los Angeles, CA, USA;* [i] *Mount Sinai Hospital, New York, NY, USA;* [j] *Department of Urology, Canisius Wilhelmina Hospital, Nijmegen, The Netherlands;* [k] *Prosper Prostate Cancer Clinics, Nijmegen/Eindhoven, The Netherlands;* [l] *Department of Urology, University of Alabama at Birmingham, Birmingham, AL, USA;* [m] *Duke University School of Medicine, Durham, NC, USA;* [n] *Turku University Central Hospital, Turku, Finland;* [o] *University of Turku, Turku, Finland;* [p] *Blue Earth Diagnostics Ltd, Oxford, UK;* [q] *Blue Earth Diagnostics Inc, Monroe Township, NJ, USA;* [r] *Division of Nuclear Medicine and Molecular Imaging, Department of Radiology and Imaging Sciences, Emory University, Atlanta, GA, USA;* [s] *Department of Urology, The University of Texas MD Anderson Cancer Center, Houston, TX, USA*

Article info

Article history:
Accepted June 20, 2023

Associate Editor:
Todd Morgan

Statistical Editor:
Melissa Assel

Abstract

Background: Radiohybrid (rh) ^{18}F-rhPSMA-7.3 is a novel high-affinity prostate-specific membrane antigen (PSMA)-targeting radiopharmaceutical for prostate cancer (PCa) imaging.
Objective: To evaluate the diagnostic performance and safety of ^{18}F-rhPSMA-7.3 in newly diagnosed PCa patients planned for prostatectomy.
Design, setting, and participants: Data on ^{18}F-rhPSMA-7.3 were reported from the phase 3 prospective, multicentre LIGHTHOUSE study (NCT04186819).
Outcome measurements and statistical analysis: Patients underwent positron emission tomography/computed tomography (PET/CT) 50–70 min after an injection of 296 MBq ^{18}F-rhPSMA-7.3. Images were interpreted locally and by three blinded independent

† The affiliation provided here represents the address at the time of the study.
[1] See Acknowledgements for group members affiliations.
* Corresponding author. The University of Texas MD Anderson Cancer Center, 1400 Pressler St, Unit Number: 1483, Houston, TX 77030, USA. Tel. +1 713 792 6536; Fax: +1 713 563 3694.
E-mail address: dssurasi@mdanderson.org (D.S. Surasi).

https://doi.org/10.1016/j.eururo.2023.06.018
0302-2838/© 2023 The Authors. Published by Elsevier B.V. on behalf of European Association of Urology. This is an open access article under the CC BY license (http://creativecommons.org/licenses/by/4.0/).

Keywords:
Prostatic neoplasms
Positron emission tomography
Prostate-specific membrane antigen
Radiohybrid prostate-specific membrane antigen

EU ACME
www.eu-acme.org/europeanurology

Please visit www.eu-acme.org/europeanurology to answer questions on-line. The EU-ACME credits will then be attributed automatically.

readers. The coprimary endpoints were patient-level sensitivity and specificity for the detection of pelvic lymph node (PLN) metastases, validated using histopathology at PLN dissection. Prespecified statistical thresholds (lower bounds of 95% confidence interval [CI]) were set at 22.5% for sensitivity and 82.5% for specificity.

Results and limitations: Of 372 patients screened, 352 had evaluable ^{18}F-rhPSMA-7.3-PET/CT and 296 (99 [33%] with unfavourable intermediate-risk [UIR] and 197 [67%] with high-/very-high-risk [VHR] PCa) subsequently underwent surgery. As per the independent reads, 23–37 (7.8–13%) patients had ^{18}F-rhPSMA-7.3–positive PLN. Seventy (24%) patients had one or more positive PLNs on histopathology. The sensitivity for PLN detection was 30% (95% CI, 19.6–42.1%) for reader 1, 27% (95% CI, 17.2–39.1%) for reader 2, and 23% (95% CI, 13.7–34.4%) for reader 3, not meeting the prespecified threshold. Specificity was 93% (95% CI, 88.8–95.9%), 94% (95% CI, 89.8–96.6%), and 97% (95% CI, 93.7–98.7%), respectively, exceeding the threshold for all readers. Specificity was high (≥92%) across both risk stratifications. Sensitivity was higher among high-risk/VHR (24–33%) than among UIR (16–21%) patients. Extrapelvic (M1) lesions were reported for 56–98/352 (16–28%) patients who underwent ^{18}F-rhPSMA-7.3-PET/CT irrespective of surgery. Verification of these (predominantly by conventional imaging) gave a verified detection rate of 9.9–14% (positive predictive value, 51–63%). No serious adverse events were observed.

Conclusions: Across all risk stratifications, ^{18}F-rhPSMA-7.3-PET/CT had high specificity, meeting the specificity endpoint. The sensitivity endpoint was not met, although higher sensitivity was noted among high-risk/VHR than among UIR patients. Overall, ^{18}F-rhPSMA-7.3-PET/CT was well tolerated, and identified N1 and M1 disease prior to surgery in newly diagnosed PCa patients.

Patient summary: In order to select the most appropriate treatment for patients with prostate cancer, it is critical to diagnose the disease burden accurately at initial diagnosis. In this study, we investigated a new diagnostic imaging agent in a large population of men with primary prostate cancer. We found it to have an excellent safety profile and to provide clinically useful information regarding the presence of disease beyond the prostate.

© 2023 The Authors. Published by Elsevier B.V. on behalf of European Association of Urology. This is an open access article under the CC BY license (http://creativecommons.org/licenses/by/4.0/).

1. Introduction

Staging of newly diagnosed prostate cancer (PCa) includes identification of both regional nodal involvement (N1) and distant metastatic disease (M1) [1]. Accurate diagnosis, particularly of extraprostatic disease, is essential for appropriate treatment decision-making and patient counselling owing to the likelihood that metastatic disease may change the planned treatment.

Until recently, bone scintigraphy and abdominal/pelvic computed tomography (CT) or magnetic resonance imaging (MRI) were the mainstay for initial staging in patients with newly diagnosed high-risk and very-high-risk (VHR) PCa, as well as in a subgroup of patients with unfavourable intermediate-risk (UIR) disease [2]. However, these conventional imaging modalities have been reported to have limited diagnostic performance in PCa staging [3,4]. Positron emission tomography (PET) can reliably identify N1 and M1 disease prior to therapy in order to stage accurately newly diagnosed patients, informing their management and ultimately improving outcomes. Two prostate-specific membrane antigen (PSMA)-targeting PET radiopharmaceuticals, ^{68}Ga-PSMA-11 and ^{18}F-DCFPyL, have gained U.S. Food and Drug Administration approval [5,6]. In addition, ^{18}F-rhPSMA-7.3 (Supplementary material [Supplementary Fig. A1]), a high-affinity PSMA-PET radiopharmaceutical, is in development as a diagnostic imaging agent for PCa. Clinical data [7] show ^{18}F-rhPSMA-7.3 to have lower average urinary excretion than ^{18}F-DCFPyL and ^{68}Ga-PSMA-11, which may facilitate improved imaging in the pelvic region. Furthermore, retrospective data from routine clinical use in Germany show that ^{18}F-rhPSMA-7.3 has superior diagnostic performance to morphological imaging for primary N staging [8].

Herein, we report the first data on the diagnostic performance and safety of ^{18}F-rhPSMA-7.3 from the phase 3 LIGHTHOUSE study (NCT04186819) investigating ^{18}F-rhPSMA-7.3 in men with newly diagnosed PCa planned to undergo radical prostatectomy (RP) with pelvic lymph node (LN) dissection (PLND). The study enrolled patients with UIR to VHR disease to address its use in a broad range of risk classifications.

2. Patients and methods

Prior to study initiation, the study protocol (Supplementary material) was approved by each study site's institutional review board/independent ethics committee. The study was conducted in accordance with the Declaration of Helsinki and the International Council on Harmonization Guidelines for Good Clinical Practice. All patients provided written informed consent.

2.1. Patients

Men (>18 yr) with biopsy-proven adenocarcinoma of the prostate and UIR-to-VHR disease classification who were scheduled to undergo RP with PLND were enrolled from 31 sites across the USA and Europe (Sup-

plementary material). The Supplementary material provides the disease risk definitions, enrolment criteria, and details of the baseline assessments. Patients received standard-of-care imaging (bone scan [^{99m}Tc-HDP and ^{99m}Tc-MDP], abdominal/pelvic CT or MRI, or chest CT as per institutional preference) as part of the baseline assessment at least 24 h before ^{18}F-rhPSMA-7.3-PET/CT.

2.2. Imaging with ^{18}F-rhPSMA-7.3-PET/CT

Patients received a target activity of 296±20% MBq ^{18}F-rhPSMA-7.3 as an intravenous bolus, with PET/CT conducted 50–70 min later. The CT acquisition was performed without intravenous contrast for anatomic localisation and attenuation correction purposes only.

This was an open-label study, and all images were evaluated initially by study site–based readers to determine whether N1 or M1 disease was detected and to inform subsequent standard-of-truth (SoT) activities. For the determination of study endpoints, all ^{18}F-rhPSMA-7.3-PET/CT images were sent to the imaging core laboratory for interpretation by three independent central PET readers (all board-certified nuclear medicine physicians with >15 yr of experience) who were blinded to all clinical information, including the local site conventional imaging and PET reads. All local and central readers received specific training on interpreting ^{18}F-rhPSMA-7.3 images.

2.3. Standard-of-care treatment

Patients received standard-of-care treatment for PCa within 60 d after ^{18}F-rhPSMA-7.3-PET/CT if the onsite read did not detect M1 disease. If M1 disease was identified by PET, verification (additional conventional imaging, biopsy, or surgery) was attempted before treatment. In patients with verified M1 disease, external beam radiation therapy could be performed instead of surgery (as per the standard of care) if deemed preferable by the patient and physician.

The regional PLND included, at a minimum, resection of lymphatic tissue for a histological analysis from the following nodal groups: hypogastric (internal iliac), external iliac, and obturator LNs. An extended LN dissection (to include presacral, perirectal, and/or common iliacs) could be performed, depending on the site standard of care. The location of the dissected material was marked to allow matching with its anatomical origin (left/right hemipelvis). Dissected LNs were sectioned and analysed by a study-site pathologist for the presence or absence of PCa according to the site's standard of care.

2.4. Standard of truth

For the assessment of endpoints related to pelvic nodal involvement, histopathology of surgically removed lymphatic tissue was the SoT. The presence of at least one PET-positive pelvic LN and one histopathologically proven LN on the same side of the pelvis was consiered a true positive (TP) at the patient level, as described in the Supplementary material (protocol Table 6).

For suspected M1 lesions, histopathology, or confirmatory conventional imaging (CT, bone scan, or MRI) was used. Confirmatory imaging of suspected M1 disease was read centrally by a panel of three SoT readers who were provided limited clinical information (age at screening, date of initial diagnosis, tumour-node-metastasis staging, Gleason Score, most recent prostate-specific antigen [PSA] level, and procedure list with start/end dates). The SoT panel reviewed all available conventional imaging and reached consensus on the nature of the PET-positive M1 lesions.

2.5. Efficacy measures

The coprimary endpoints were patient-level sensitivity and specificity of ^{18}F-rhPSMA-7.3 for the detection of pelvic LN metastases, where sensitivity = TP/(TP + FN) and specificity = TN/(TN + FP).

The secondary endpoints included the following:

1. Patient-level positive predictive value (PPV) of ^{18}F-rhPSMA-7.3-PET/CT findings (as determined by the central blinded image evaluation [BIE]) for detecting pelvic LN metastases (compared with histopathology), where PPV = TP/(TP + FP)
2. Patient-level negative predictive value (NPV) for the detection of pelvic LN metastases compared with histopathology. For this particular analysis, a false-negative (FN) patient was defined as having one or more FN regions (right or left hemipelvis), regardless of any coexisting true negatives (TNs), where NPV = TN/(TN + FN)
3. Patient-level ^{18}F-rhPSMA-7.3-PET/CT verified detection rate (VDR) for M1 disease (as determined by BIE), where VDR = (TP)/(TP + FP + BIE negative)
4. Patient-level ^{18}F-rhPSMA-7.3-PET/CT PPV (as determined by BIE) for M1 lesions (compared with histopathology or confirmatory imaging)
5. Safety assessments

Further subgroup analyses of the endpoints were conducted with patients stratified by PCa risk category and International Society of Urological Pathology (ISUP) grade group (GG).

2.6. Safety

All patients were monitored for the frequency of adverse events (AEs), graded according to Common Terminology Criteria for Adverse Events version 5 [9], from informed consent until last visit. Vital sign monitoring was conducted at screening and also before and after ^{18}F-rhPSMA-7.3-PET/CT.

2.7. Statistical analysis

Both coprimary endpoints were summarised as a percentage and two-sided exact 95% confidence interval (95% CI) for each of the three readers and for the majority read interpretation (agreement of two or more readers). The TP, false-positive (FP), TN, and FN regions were categorised using the right and left hemipelvis regional classification method detailed in the protocol. For the primary analysis, patients with one TP region were categorised as TP. The primary analysis included patients as FN if they had only one positive region by histopathology and it was missed by PET.

Performance goals for the lower bound of the 95% CI of 22.5% for sensitivity and 82.5% for specificity were selected based on the low sensitivity but high specificity of other PSMA-PET ligands used for N staging. A total sample size of ~375 patients was planned in order to obtain 300 evaluable patients for the primary endpoint. This assumed sensitivity of 40% for detecting N1 disease [10]; a sample size of 75 positive cases would, therefore, provide 90% power to reject the 22.5% performance goal. Assuming specificity of 90%, a sample size of 225 negative cases would provide 90% power to reject the 82.5% performance goal. The analyses for sensitivity and specificity were performed using one-sided 0.025 exact binomial tests.

The safety analysis evaluated all patients who received ^{18}F-rhPSMA-7.3. The efficacy population comprised all patients who underwent ^{18}F-rhPSMA-7.3-PET/CT and subsequent RP and PLND, and was used to assess the coprimary endpoints. An extended population comprising all patients who underwent ^{18}F-rhPSMA-7.3-PET/CT irrespective of subsequent surgery was used to analyse M1-related efficacy.

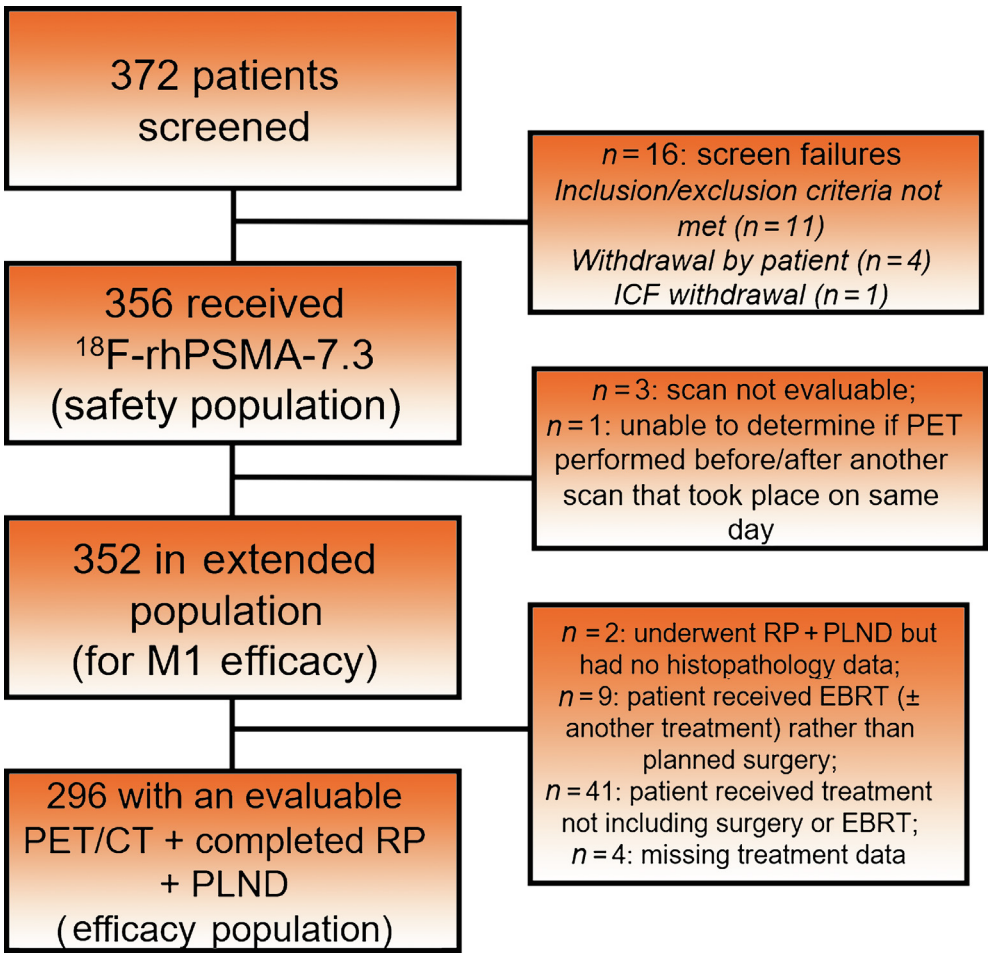

Fig. 1 – STARD flow diagram of study participants. CT = computed tomography; EBRT = external beam radiation therapy; ICF = informed consent form; LN = lymph node; PET = positron emission tomography; PLND = pelvic lymph node dissection; RP = radical prostatectomy.

3. Results

As shown in Figure 1, 372 patients were screened between March 2020 and March 2021. Table 1 presents the baseline characteristics for both the efficacy population (n = 296) and the extended population (n = 352).

Pelvic LN and metastatic findings by ^{18}F-rhPSMA-7.3 were broadly consistent by local site read and BIE (Table 2).

3.1. Pelvic LN sampling

Pelvic LN sampling data were recorded for 295/296 patients in the efficacy population. One patient underwent PLND, but the number of LNs sampled was not recorded. A median of 16 (interquartile range, 9–23) LNs were sampled per patient. Overall, 70 patients (24%) had at least one positive pelvic LN on histopathology.

3.2. Detection of pelvic LN metastases

3.2.1. Sensitivity

Patient-level sensitivity among the efficacy population (n = 296) ranged across readers from 23% to 30% (majority read, 24%; Table 3). The lower bound 95% CI ranged from 13.7% to 19.6%, not exceeding the prespecified statistical threshold (p = 0.09–0.5). In a subgroup with UIR disease (n = 99), the sensitivity ranged from 16% to 21% (majority read, 16%) and was higher (24–33%; majority read, 27%) among patients with high-risk or VHR disease (n = 197).

Patient-level sensitivity was higher among patients with ISUP GG 5 (38–52% across readers) than among those with lower GG (Supplementary material). Sensitivity remained broadly consistent across PSA ranges (Supplementary material).

3.2.2. Specificity

Patient-level specificity ranged from 93% to 97% across readers (majority read, 96%), with the lower bound 95% CI ranging from 88.8% to 93.7%, exceeding the prespecified statistical threshold for all three readers (p < 0.001) and meeting the coprimary endpoint (Table 3). Specificity ranged from 94% to 99% (majority read, 98%) in the UIR subgroup and from 92% to 96% (majority read, 95%) among the patients with high-risk/VHR disease.

Specificity was broadly high irrespective of GG or baseline PSA (Supplementary material).

3.2.3. PPV and NPV

Among the efficacy population, the patient-level PPV (compared with surgical histopathology) was 57–70% across

Table 1 – Patients' baseline characteristics and ^{18}F-rhPSMA-7.3-PET/CT details

	Extended population (for M1 efficacy; *N* = 352)	Efficacy population (*N* = 296)
Age (yr)		
Median	65	65
IQR	60–70	60–70
Time since initial diagnosis (mo)		
Median	1	1
IQR	0–2	0–2
Grade group, *n* (%)		
1	6 (1.7)	5 (1.7)
2	50 (14)	42 (14)
3	108 (31)	91 (31)
4	86 (24)	78 (26)
5	102 (29)	80 (27)
cT1 stage, *n* (%)		
T1	144 (41)	121 (41)
T2	131 (37)	112 (38)
T3	54 (15)	45 (15)
T4	2 (0.6)	1 (0.3)
TX or missing	21 (6.0)	17 (5.7)
PSA at last measurement (ng/ml)		
Median	8.8	8.5
IQR	6.0–15.8	5.8–14.7
Risk stratification, *n* (%)		
Unfavourable intermediate	114 (32)	99 (33)
Baseline conventional imaging [a]	*N* = 351	*N* = 295
Pelvic LN, *n* (%)		
Positive	21 (6.0)	12 (4.1)
M1 (extrapelvic site), *n* (%)		
Positive	20 (5.7)	14 (4.7)
^{18}F-rhPSMA-7.3-PET/CT		
Administered activity (MBq)		
Median	307.3	308.0
IQR	296.0–321.9	296.7–322.0

CT = computed tomography; IQR = interquartile range; LN = lymph node; MRI = magnetic resonance imaging; PET = positron emission tomography; PSA = prostate-specific antigen.

[a] Data missing for one patient. In the extended population, 272 patients had a bone scan, 211 had a CT scan, and 150 had MRI. In the efficacy population, 225 patients had a bone scan, 175 had a CT scan, and 134 had MRI.

readers (majority read, 65%). NPV ranged from 80% to 81%, with a majority read of 80% (Table 4).

3.3. Detection of M1 lesions

Extrapelvic lesions were documented among an extended population comprising all patients who had ^{18}F-rhPSMA-7.3-PET/CT irrespective of surgery (*n* = 352). Figure 2 presents images of extrapelvic lesions detected with ^{18}F-rhPSMA-7.3-PET/CT. As detailed in the Supplementary material, extrapelvic M1 lesions were found in 56–98 (16–28%) patients, resulting in an M1 VDR of 9.9–14% and patient-level PPV of 51–63%, using predominantly confirmatory conventional imaging as the gold standard.

3.4. Safety data

Overall, 28 of the 356 patients in the safety population (7.9%) experienced a total of 33 treatment-emergent AEs, none of which were serious. Nine (2.5%) patients experienced a total of ten treatment-emergent AEs possibly related to ^{18}F-rhPSMA-7.3. Injection site pain was experienced by three (0.8%) patients. Peripheral swelling, diarrhoea, nausea, hyperkalaemia, arthralgia, dysgeusia, and hypertension were each reported for one (0.3%) patient.

4. Discussion

LIGHTHOUSE evaluated the diagnostic performance and safety of the novel PSMA-targeting radiopharmaceutical ^{18}F-rhPSMA-7.3 in a large, diverse population of men with newly diagnosed UIR-to-VHR PCa. Consistent with previous studies of ^{18}F-rhPSMA-7.3, no significant safety signals were identified [7,11,12].

The coprimary endpoint of patient-level specificity for the detection of N1 disease was met, as the prespecified statistical success threshold was exceeded by each of the three independent PET readers ($p < 0.001$) and for the majority read ($p < 0.001$). The prespecified statistical threshold for sensitivity was not exceeded by the readers, and thus the coprimary sensitivity endpoint was not met.

Sensitivity is a known challenge for the existing PSMA-PET agents [10,13], particularly for lesions <5 mm, which can be under the test's detection limit [14–16]. Lesions are considered positive on histopathology irrespective of size. Thus, since PET will always be less sensitive than the

Table 2 – Findings of ^{18}F-rhPSMA-7.3 by local site read and blinded image evaluation

	Local read	Blinded image evaluation			
		Reader 1	Reader 2	Reader 3	Majority read
Extended population (*n* = 352)	N0 = 276	N0 = 291	N0 = 301	N0 = 308	N0 = 305
	N1 = 76	N1 = 61	N1 = 51	N1 = 44	N1 = 47
	M0 = 289	M0 = 296	M0 = 254	M0 = 289	M0 = 291
	M1 = 63	M1 = 56	M1 = 98	M1 = 63	M1 = 61
Efficacy population (*n* = 296)	N0 = 250	N0 = 259	N0 = 263	N0 = 273	N0 = 270
	N1 = 46	N1 = 37	N1 = 33	N1 = 23	N1 = 26
	M0 = 263	M0 = 268	M0 = 231	M0 = 258	M0 = 263
	M1 = 33	M1 = 28	M1 = 65	M1 = 38	M1 = 33
	M1a = 10	M1a = 7	M1a = 4	M1a = 6	
	M1b = 17	M1b = 16	M1b = 55	M1b = 27	
	M1c = 6	M1c = 5	M1c = 6	M1c = 5	

Table 3 – Patient-level sensitivity and specificity for the detection of pelvic LN metastases in the efficacy population

	Reader 1	Reader 2	Reader 3	Majority read
Sensitivity				
All patients (*n* = 296)	30% (21/70)	27% (19/70)	23% (16/70)	24% (17/70)
95% CI	19.6–42.1%	17.2–39.1%	13.7–34.4%	14.8–36.0%
***p* value**	0.09	0.2	0.5	0.4
UIR (*n* = 99)	21% (4/19)	16% (3/19)	21% (4/19)	16% (3/19)
95% CI	6.1–45.6%	3.4–39.6%	6.1–45.6%	3.4–39.6%
High risk or VHR (*n* = 197)	33% (17/51)	31% (16/51)	24% (12/51)	27% (14/51)
95% CI	20.8–47.9%	19.1–45.9%	12.8–37.5%	15.9–41.7%
Specificity				
All patients (*n* = 296)	93% (210/226)	94% (212/226)	97% (219/226)	96% (217/226)
95% CI	88.8–95.9%	89.8–96.6%	93.7–98.7%	92.6–98.2%
***p* value**	<0.001	<0.001	<0.001	<0.001
UIR (*n* = 99)	94% (75/80)	95% (76/80)	99% (79/80)	98% (78/80)
95% CI	86.0–97.9%	87.7–98.6%	93.2–100.0%	91.3–99.7%
High risk or VHR (*n* = 197)	92% (135/146)	93% (136/146)	96% (140/146)	95% (139/146)
95% CI	86.9–96.2%	87.8–96.7%	91.3–98.5%	90.4–98.1%

95% CI = 95% confidence interval; UIR = unfavourable intermediate-risk disease; VHR = very high risk.

Table 4 – Patient-level PPV and NPV for the detection of pelvic LN metastases

	Reader 1 *N* = 296	Reader 2 *N* = 296	Reader 3 *N* = 296	Majority read *N* = 296
Patient-level PPV for the detection of pelvic LN metastases				
Number of patients with PET-positive finding in pelvic LN (TP + FP)	37	33	23	26
True positive	21 (57%)	19 (58%)	16 (70%)	17 (65%)
False positive	16 (43%)	14 (42%)	7 (30%)	9 (35%)
PPV	57% (21/37)	58% (19/33)	70% (16/23)	65% (17/26)
[95% CI]	[39.5–72.9%]	[39.2–74.5%]	[47.1–86.8%]	[44.3–82.8%]
Patient-level NPV for the detection of pelvic LN metastases				
Number of patients with PET-negative finding in pelvic LN (TN + FN)	284	287	289	287
True negative	231 (81%)	232 (81%)	231 (80%)	230 (80%)
False negative	53 (19%)	55 (19%)	58 (20%)	57 (20%)
NPV	81% (231/284)	81% (232/287)	80% (231/289)	80% (230/287)
[95% CI][a]	[76.3–85.7%]	[75.8–85.2%]	[74.8–84.4%]	[75.0–84.6%]

95% CI = 95% confidence interval; FN = false negative; FP = false positive; LN = lymph node; NPV = negative predictive value; PET = positron emission tomography; PPV = positive predictive value; TN = true negative; TP = true positive.
[a] For the evaluation of NPV, an FN patient was defined as having at least one FN region (right or left pelvis), regardless of any coexisting TN findings.

histopathology SoT, some degree of FN results is inevitable in trials of this type because of the lack of consideration of a size threshold to define a positive lesion that should be detectable by ^{18}F-rhPSMA-PET. As the size of lesions identified or missed by ^{18}F-rhPSMA-7.3-PET/CT was not captured routinely in the present study, future studies should be conducted to determine the lower limit of detection.

The LIGHTHOUSE study enrolled patients across a broad range of disease risk stratifications that resembled a real-world population of primary PCa patients who would be candidates for surgery, with one-third of all enrolled patients having UIR disease. Moreover, only 4.1% of the efficacy population had baseline conventional imaging that was positive for pelvic LN metastases. In contrast, the PSMA phase 3 registration trials to date have focused on high-risk patients; OSPREY [10] recruited only high-risk patients and the ^{68}Ga-PSMA-11 trial [13] recruited just 18% of intermediate-risk patients in the surgery cohort, with relatively higher rates of enrolled patients with positive baseline conventional imaging for N1/M1 disease in OSPREY [17,18]. Commensurate with the risk category and known correlation of PSMA expression with disease aggressiveness [19], lower-risk patients are expected to have smaller lesions expressing lower levels of PSMA, potentially below the resolution of PET, which would have affected the endpoints. Indeed, when considering data from patients with only high-risk or VHR disease, sensitivity increases to 27% relative to the 16% observed in patients with UIR disease. Further support is added from the observation that sensitivity is meaningfully higher in patients with GG 5 than in other groups.

Despite the low sensitivity, patient-level NPV was broadly high across all readers, suggesting that clinicians can have a good level of confidence in a negative scan. NPV is comparable with other agents [10,13] despite the noted differences in patient populations. Nonetheless, it is important to note that negative PSMA-PET in this population is not intended to change the current risk-based standard-of-care approach of conducting PLND with RP. Currently, for CT and MRI, 8–10 mm is considered the size threshold for pathological LNs [4]. Microscopic metastatic deposits in pelvic LNs below this size can be identified by a histopathological examination only, and therefore, the current risk-based approach used by urologists to decide whether to perform PLND will necessarily continue. The use of PSMA-PET in this population can help inform accurate preoperative patient counselling, and the identification of any PSMA-positive nodes not seen on conventional imag-

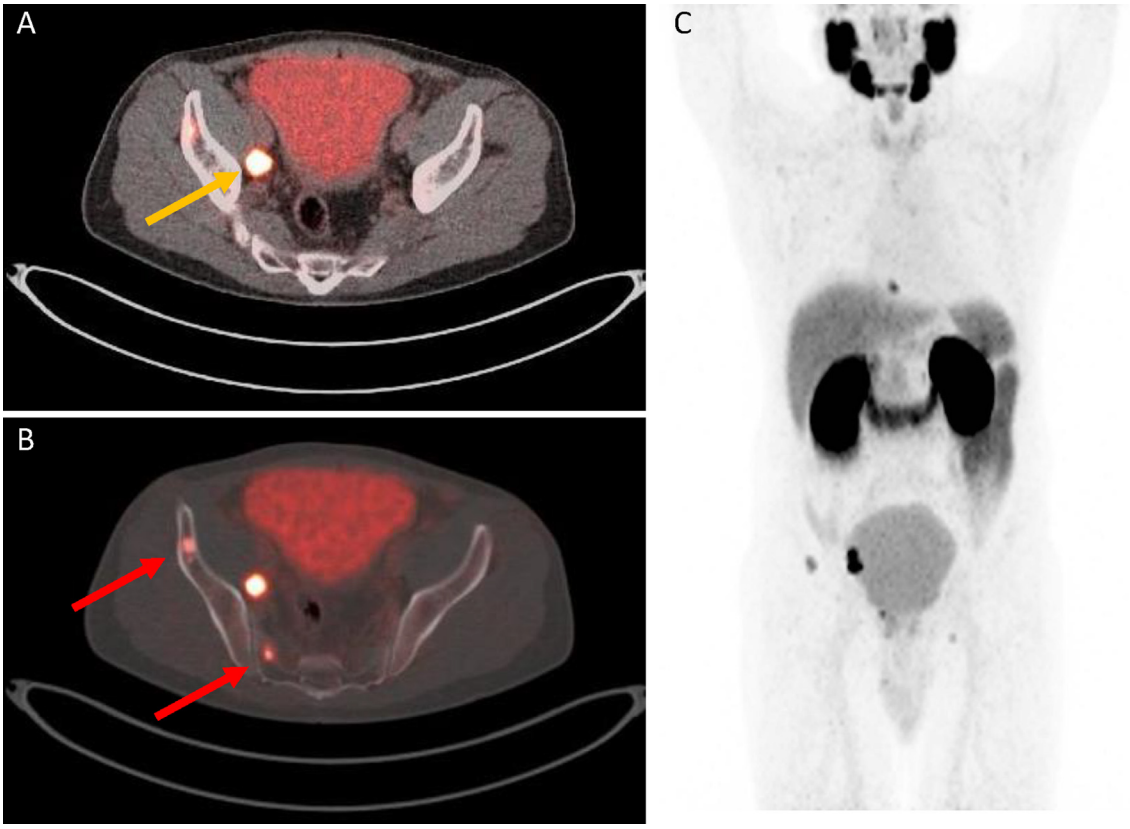

Fig. 2 – Images captured from a patient in LIGHTHOUSE. (A and B) Fused ^{18}F-rhPSMA-7.3-PET/CT images and (C) MIP (SUV 0–10) of a 66-yr-old patient initially presenting with unfavourable intermediate-risk PCa (Gleason 4 + 3, PSA 11.0 ng/ml, cT2), upstaged by findings of ^{18}F-rhPSMA-7.3–avid pelvic LN (Fig. 2A, yellow arrow) and multiple bone metastases, for example, in the sacrum (Fig. 2B, red arrows) and T10 vertebra (Fig. 2C, midline above the liver). The bone metastases were subsequently verified as true positive on CT. CT = computed tomography; LN = lymph node; MIP = maximum intensity projection; PCa = prostate cancer; PET = positron emission tomography; PSA = prostate-specific antigen; SUV = standardised uptake value.

ing that are outside the planned surgical field could allow adjustment of the field prior to surgery.

Patient-level N1 PPV was moderately high but was impacted by a degree of FP lesions. One explanation is that LNs identified on ^{18}F-rhPSMA-7.3-PET were not part of the standard nodal dissection at surgery. This was anticipated to a degree, given the known variability in practice of PLND extent, propensity of LN metastases to be missed during PLND [20,21], the minimum study stipulation for regional PLND, and flexibility afforded to sites to otherwise proceed with dissection extent as per the standard of care.

Although the prevalence of M1 lesions among this newly diagnosed population, one-third of which had UIR disease, was expected to be low, 16–28% of patients had ^{18}F-rhPSMA-7.3–positive M1 lesions. This conferred a VDR of 9.9–14% and a moderately high PPV of 51–63%. The skeletal system is the most common site of distant metastatic spread in PCa [22], and our data showing bone to be the most frequent site for ^{18}F-rhPSMA-7.3 M1 detections (M1b detection rate, 13%) agree with this. However, high uptake of PSMA-targeted PET radiopharmaceuticals in various benign bone pathologies, such as healing fractures [23,24], Paget's disease [25–27], and fibrous dysplasia [28], can lead to FP findings that mimic PCa metastases. Although verification of M1 lesions as TPs was predominantly by conventional imaging (85% [29/34] by majority read), which likely led to a number of "false FPs", our data show that 50% of ^{18}F-rhPSMA-7.3–avid bone lesions were verified as TPs. Thus, by majority read, ^{18}F-rhPSMA-7.3 identified a TP bone lesion in 6.3% of patients. The identification of confirmed distant metastatic disease prior to RP and PLND may spare such patients undergoing surgery that might be futile in favour of a switch to multimodality and/or systemic treatments.

The utility of PSMA-PET agents can be limited by high urinary bladder activity, resulting in poor delineation of the local tumour and some pelvic LNs [29–31]. As the average urinary excretion of ^{18}F-rhPSMA-7.3 is lower than that of the currently approved agents [7], a potential exists for improved imaging in the pelvic region and basal prostate. Data from a retrospective analysis of the clinical use of ^{18}F-rhPSMA-7.3 show good distinction between the primary tumour and background bladder activity [8], as is noted visually in the images here and from the SPOTLIGHT study of patients with recurrent PCa [12]. A further distinction of ^{18}F-rhPSMA-7.3 from existing PSMA-PET agents is the rhPSMA platform's potential for the development of true theranostics, through labelling with ^{18}F for diagnostic imaging or with alpha- or beta-emitters for therapeutic use [32]. Thus, as these have similar chemical structures

to the therapeutic agents, rhPSMA diagnostic agents may be ideally suited to identify patients who are suitable for radioligand therapy with any future rhPSMA therapeutics. Phase 1/2 trials of rhPSMA radioligand therapy are currently underway (NCT05413850), and recent preclinical data show ^{177}Lu-labelled rhPSMA to perform favourably, with a markedly improved tumour:kidney uptake ratio and suppression of tumour growth relative to ^{177}Lu-PSMA-I&T [33].

There are a number of limitations to the present study. Firstly, as LIGHTHOUSE was not designed to compare ^{18}F-rhPSMA-7.3-PET with existing PSMA-PET agents, and in the absence of head-to-head comparisons, caution should be applied in drawing comparisons based on individual trial data owing to the impact that differing patient populations, scanning procedures, readers, and the differences in SoT protocols have on reported outcomes. Furthermore, as histopathology data from pelvic LN sampling show, the prevalence of N1 disease is fairly low at 24% in this population, which might have affected the PPV estimates. Additionally, as expected, the prevalence of M1 lesions among this newly diagnosed population, one-third of whom had UIR disease, was low, impacting the estimates of M1 VDR and PPV. Lastly, while ^{18}F-rhPSMA-7.3-PET may provide high specificity for N1 disease and provide useful data on the presence of M1 disease in these newly diagnosed patients, which could inform future treatment, outcomes were not measured and the impact of this on patients is unknown.

5. Conclusions

In this phase 3 study comprising the broadest population of primary PCa patients in its class, ^{18}F-rhPSMA-7.3 was well tolerated. The specificity endpoint was met, with high specificity noted across all risk stratifications. The coprimary endpoint of sensitivity was not met. However, lower sensitivity is common within the class of PSMA-targeted diagnostic radiopharmaceuticals and likely related to the enrolled population. Overall, ^{18}F-rhPSMA-7.3-PET/CT provides clinically useful information regarding the identification of both N1 and M1 disease prior to surgery.

***Author contributions*:** Devaki Shilpa Surasi had full access to all the data in the study and takes responsibility for the integrity of the data and the accuracy of the data analysis.

Study concept and design: Davis, Chau, Chapin, Schuster.
Acquisition of data: Surasi, Preston, Helfand, Josephson, Tewari, Rais-Bahrami, Koontz, Maurer, Eiber, Bostrom, Somford, Schuster, Chapin.
Analysis and interpretation of data: Surasi, Preston, Helfand, Josephson, Rais-Bahrami, Koontz, Maurer, Eiber, Chau, Davis, Bostrom, Somford, Schuster, Chapin.
Drafting of the manuscript: Surasi, Preston, Helfand, Josephson, Tewari, Rais-Bahrami, Koontz, Maurer, Eiber, Bostrom, Somford, Chau, Davis, Schuster, Chapin.
Critical revision of the manuscript for important intellectual content: Surasi, Preston, Helfand, Josephson, Tewari, Rais-Bahrami, Koontz, Maurer, Eiber, Bostrom, Somford, Chau, Davis, Schuster, Chapin.
Statistical analysis: Chau.
Obtaining funding: None.
Administrative, technical, or material support: Davis.
Supervision: Davis, Chapin.
Other: None.

Financial disclosures: Devaki Shilpa Surasi certifies that all conflicts of interest, including specific financial interests and relationships and affiliations relevant to the subject matter or materials discussed in the manuscript (eg, employment/affiliation, grants or funding, consultancies, honoraria, stock ownership or options, expert testimony, royalties, or patents filed, received, or pending), are the following: Devaki Shilpa Surasi reports research support from Blue Earth Diagnostics for an investigator-initiated study. Matthias Eiber has a patent application for rhPSMA, and also reports (outside the submitted work) consultancy/speaker fees from Blue Earth Diagnostics Ltd, Novartis/AAA, Telix, Bayer, RayzeBio, Point Biopharma, Eckert-Ziegler, and Janssen Pharmaceuticals; research funding from Blue Earth Diagnostics Ltd and Bayer; and image review contracts for Parexel and Bioclinica. Tobias Maurer reports personal fees from Bayer, Sanofi-Aventis, Astellas, and Phillips Advanced Accelerator (speakers bureau), and consultation fees from Applications International S.A., Novartis, Telix, ROTOP Pharma, GEMoAb, Astellas, Axiom, Blue Earth Diagnostics, and ABX. Diederik M. Somford reports consultancy fees from Astellas, Janssen, Bayer, MSD, and Ipsen; research grant/funding (institution) from Astellas, Besins, and Dutch Cancer Society; and contracted research roles (institution) for Janssen, Eli Lilly, Astellas, Blue Earth Diagnostics, Bayer, SPL Medical, and QED Therapeutics. Soroush Rais-Bahrami reports research support from Blue Earth Diagnostics, Astellas, and Varian, and consultancy fees from Blue Earth Diagnostics, Progenics, Genomic Health Inc, Intuitive Surgical, UroViu, and Bayer Healthcare. Bridget F. Koontz is the vice chair of NRG Oncology Ancillary Projects Committee and an NCI GU Steering Committee member; has participated in advisory boards for Mirrors of Medicine, Rythera Therapeutics, and Blue Earth Diagnostics; and reports consultancy fees from Rythera Therapeutics and Blue Earth Diagnostics. Peter J. Bostrom reports a research grant from Profound Inc., and consultancy/speaker fees from Astra Zeneca, Faron Pharmaceuticals, Astellas, and Janssen. Albert Chau and Phillip Davis are employees/consultants of Blue Earth Diagnostics. David M. Schuster reports consultancy fees from Syncona, AIM Specialty Health, Global Medical Solutions Taiwan, and Progenics Pharmaceuticals, Inc., and research funding (institution) from Blue Earth Diagnostics Ltd, Nihon MediPhysics Co Ltd, Telix Pharmaceuticals (US) Inc., Advanced Accelerator Applications, FUJIFILM Pharmaceuticals U.S. A. Inc., and Amgen Inc. Mark A. Preston, David Josephson, Ashutosh K. Tewari, Brian T. Helfand, and Brian F. Chapin have no conflicts to report.

***Funding/Support and role of the sponsor*:** The LIGHTHOUSE study was sponsored by Blue Earth Diagnostics Ltd, Oxford, UK.

***Acknowledgements*:** Contributors: in addition to the authors, the following individuals are members of the LIGHTHOUSE Study Group: Mohamad Allaf (Johns Hopkins University, Baltimore, MD, USA), Gerald Andriole (Washington University School of Medicine, St. Louis, MO, USA), Ryan J. Avery (Northwestern University, Chicago, IL, USA), Norbert Avril (Cleveland Medical Center, Cleveland, OH, USA), Helen Barker (Blue Earth Diagnostics Ltd, Oxford, UK), Laurence Belkoff (MidLantic Urology, Bala Cynwyd, PA, USA), Lars Budäus (Martini-Klinik, University Hospital Hamburg-Eppendorf, Hamburg, Germany), Michael L. Cher (Karmanos Cancer Center, Detroit, MI, USA), Diane Chisholm (Blue Earth Diagnostics Ltd, Oxford, UK), Matthew F. Covington (University of Utah Health, Salt Lake City, UT, USA), Ian Cox (Blue Earth Diagnostics Ltd, Oxford, UK), Michael Ferrandino (Duke University Medical Center, Durham, NC,

USA), Mark T. Fleming (Virginia Oncology Associates, Norfolk, VA, USA), Dinko Franceschi (Stony Brook University, Stony Brook, NY, USA), Peter Gardiner (Blue Earth Diagnostics Inc., Monroe Township, NJ, USA), Benjamin Gartrell (Montefiore Medical Center, Bronx, NY, USA), David Gauden (Blue Earth Diagnostics Ltd, Oxford, UK), Ergela Hasa (Klinikum rechts der Isar, Technische Universität München, Munich, Germany), Rick Hermsen (Canisius Wilhelmina Hospital, Nijmegen, The Netherlands), Thomas Horn (Klinikum rechts der Isar, Technische Universität München, Munich, Germany), Pooya Iranpour (Richard L Roudebush VA Medical Center, Indianapolis, IN, USA), Heather Jacene (Brigham and Women's Hospital, Boston, MA, USA), Isuru Jayaratna (Queens Hospital Center, Queens, NY, USA), Shreyas S. Joshi (Emory University, Atlanta, GA, USA), Matthew Kay (University of Arizona Medical Center, Tucson, AZ, USA), Lale Kostakoglu (University of Virginia, Health Science Center, Charlottesville, VA, USA), Phillip Kuo (Invicro, Needham, MA, USA), William Lavely (Northside Hospital, Atlanta, GA, USA), Mary Lokuta (Blue Earth Diagnostics Inc., Monroe Township, NJ, USA), Benjamin Lowentritt (Chesapeake Urology Research Associates, Towson, MD, USA), Matthew P. Miller (Blue Earth Diagnostics Ltd, Oxford, UK), Jeffrey W. Nix (University of Alabama at Birmingham, Birmingham, AL, USA), Kenneth Ogan (Emory University, Atlanta, GA, USA), Ross Penny (Blue Earth Diagnostics Ltd, Oxford, UK), Morand Piert (University of Michigan, Ann Arbor, MI, USA), Andrei Purysko (Cleveland Clinic, Cleveland, OH, USA), Gregory Ravizzini (MD Anderson, Houston, TX, USA), Daniel Saltzstein (Urology San Antonio, San Antonio, TX, USA), Bital Savir-Baruch (Loyola University, Chicago, IL, USA), Barry A. Siegel (Washington University School of Medicine, St. Louis, MO, USA), Thomas Steuber (Martini-Klinik, University Hospital Hamburg-Eppendorf, Hamburg, Germany), Przemyslaw Twardowski (John Wayne Cancer Institute, Santa Monica, CA, USA), Edward Uchio (University of California Irvine Medical Center, Orange, CA, USA), Gary A. Ulaner (Hoag Memorial Hospital, Newport Beach, CA, USA), Jenna M. Wixom (MD Anderson, Houston, TX, USA), Don Yoo (Brown University, Providence, RI, USA), and Katherine Zukotynski (McMaster University, Ontario, Canada). Dr Catriona Turnbull (Blue Earth Diagnostics Ltd) provided writing support.

Peer Review Summary

Peer Review Summary and Supplementary data to this article can be found online at https://doi.org/10.1016/j.eururo.2023.06.018.

References

[1] Union for International Cancer Control. TNM classification of malignant tumours. 2022. https://www.uicc.org/resources/tnm.
[2] NCCN. NCCN clinical practice guidelines in oncology: prostate cancer. Version 1.2022. 2021. https://www.nccn.org/professionals/physician_gls/pdf/prostate.pdf.
[3] Chong A, Hwang I, Ha JM, et al. Application of bone scans for prostate cancer staging: which guideline shows better result? Can Urol Assoc J 2014;8:E515–9.
[4] Hovels AM, Heesakkers RA, Adang EM, et al. The diagnostic accuracy of CT and MRI in the staging of pelvic lymph nodes in patients with prostate cancer: a meta-analysis. Clin Radiol 2008;63:387–95.
[5] FDA. FDA approves second PSMA-targeted PET imaging drug for men with prostate cancer. 2021. https://www.fda.gov/drugs/drug-safety-and-availability/fda-approves-second-psma-targeted-pet-imaging-drug-men-prostate-cancer.
[6] FDA. FDA approves first PSMA-targeted PET imaging drug for men with prostate cancer. 2020. https://www.fda.gov/news-events/press-announcements/fda-approves-first-psma-targeted-pet-imaging-drug-men-prostate-cancer.
[7] Tolvanen T, Kalliokoski KK, Malaspina S, et al. Safety, biodistribution and radiation dosimetry of ^{18}F-rhPSMA-7.3 in healthy adult volunteers. J Nucl Med 2021;62:679–84.
[8] Langbein T, Wang H, Rauscher I, et al. Utility of ^{18}F-rhPSMA-7.3 positron emission tomography for imaging of primary prostate cancer and pre-operative efficacy in N-staging of unfavorable intermediate to very high-risk patients validated by histopathology. J Nucl Med 2022;63:1334–42.
[9] NCI. Common Terminology Criteria for Adverse Events (CTCAE) version 5.0. 2017. https://ctep.cancer.gov/protocoldevelopment/electronic_applications/docs/ctcae_v5_quick_reference_8.5x11.pdf.
[10] Pienta KJ, Gorin MA, Rowe SP, et al. A phase 2/3 prospective multicenter study of the diagnostic accuracy of prostate specific membrane antigen PET/CT with ^{18}F-DCFPyL in prostate cancer patients (OSPREY). J Urol 2021;206:52–61.
[11] Malaspina S, Taimen P, Kallajoki M, et al. Uptake of ^{18}F-rhPSMA-7.3 in PET imaging of prostate cancer – a phase 1 proof-of-concept study. Cancer Biother Radiopharm 2022;37:205–13.
[12] Jani AB, Ravizzini G, Gartrell BA, et al. Diagnostic performance and safety of 18F-rhPSMA-7.3 PET in men with suspected prostate cancer recurrence: results from a phase 3, prospective, multicenter study (SPOTLIGHT). J Urol 2023. https://doi.org/10.1097/JU.0000000000003493, In press.
[13] Hope TA, Eiber M, Armstrong WR, et al. Diagnostic accuracy of ^{68}Ga-PSMA-11 PET for pelvic nodal metastasis detection prior to radical prostatectomy and pelvic lymph node dissection: a multicenter prospective phase 3 imaging trial. JAMA Oncol 2021;7:1635–42.
[14] Jansen BHE, Bodar YJL, Zwezerijnen GJC, et al. Pelvic lymph-node staging with ^{18}F-DCFPyL PET/CT prior to extended pelvic lymph-node dissection in primary prostate cancer—the SALT trial. Eur J Nucl Med Mol Imaging 2021;48:509–20.
[15] Petersen LJ, Nielsen JB, Langkilde NC, et al. ^{68}Ga-PSMA PET/CT compared with MRI/CT and diffusion-weighted MRI for primary lymph node staging prior to definitive radiotherapy in prostate cancer: a prospective diagnostic test accuracy study. World J Radiol 2020;38:939–48.
[16] Budaus L, Leyh-Bannurah SR, Salomon G, et al. Initial experience of ^{68}Ga-PSMA PET/CT imaging in high-risk prostate cancer patients prior to radical prostatectomy. Eur Urol 2016;69:393–6.
[17] Progenics Pharmaceuticals Inc. Study of ^{18}F-DCFPyL PET/CT imaging in patients with prostate cancer (OSPREY). ClinicalTrials.gov identifier: NCT02981368. Updated August 9, 2021. https://clinicaltrials.gov/ct2/show/study/NCT02981368.
[18] U.S. Food and Drug Administration. Center for Drug Evaluation and Research. NDA 214793 / Piflufolastat F 18 (PYLARIFY): multidisciplinary review and evaluation. https://www.accessdata.fda.gov/drugsatfda_docs/nda/2021/214793Orig1s000MultidisciplineR.pdf.
[19] Ross JS, Sheehan CE, Fisher HA, et al. Correlation of primary tumor prostate-specific membrane antigen expression with disease recurrence in prostate cancer. Clin Cancer Res 2003;9:6357–62.
[20] Lunger L, Steinhelfer L, Korn P, et al. Prostate-specific membrane antigen-radioguided surgery facilitates pelvic lymph node dissection during radical prostatectomy for the treatment of locally advanced prostate cancer with regional lymph node metastases. Eur Urol Oncol 2023;6:95–8.
[21] Hall WA, Paulson E, Davis BJ, et al. NRG Oncology Updated International Consensus atlas on pelvic lymph node volumes for intact and postoperative prostate cancer. Int J Radiat Oncol Biol Phys 2021;109:174–85.
[22] Bubendorf L, Schöpfer A, Wagner U, et al. Metastatic patterns of prostate cancer: an autopsy study of 1,589 patients. Hum Pathol 2000;31:578–83.
[23] Gykiere P, Goethals L, Everaert H. Healing sacral fracture masquerading as metastatic bone disease on a ^{68}Ga-PSMA PET/CT. Clin Nucl Med 2016;41:e346–7.
[24] Vamadevan S, Le K, Bui C, Mansberg R. Incidental PSMA uptake in an undisplaced fracture of a vertebral body. Clin Nucl Med 2017;42:465–6.
[25] Rowe SP, Deville C, Paller C, et al. Uptake of ^{18}F-DCFPyL in Paget's disease of bone, an important potential pitfall in clinical interpretation of PSMA PET studies. Tomography 2015;1:81–4.
[26] Bourgeois S, Gykiere P, Goethals L, Everaert H, De Geeter FW. A specific uptake of ^{68}Ga-PSMA in Paget disease of the bone. Clinical Nucl Med 2016;41:877–8.

[27] Blazak JK, Thomas P. Paget disease: a potential pitfall in PSMA PET for prostate cancer. Clin Nucl Med 2016;41:699–700.
[28] De Coster L, Sciot R, Everaerts W, et al. Fibrous dysplasia mimicking bone metastasis on ^{68}Ga-PSMA PET/MRI. Eur J Nucl Med Mol Imaging 2017;44:1607–8.
[29] Fendler WP, Eiber M, Beheshti M, et al. ^{68}Ga-PSMA PET/CT: Joint EANM and SNMMI procedure guideline for prostate cancer imaging: version 1.0. Eur J Nucl Med Mol Imaging 2017;44:1014–24.
[30] Heusser T, Mann P, Rank CM, et al. Investigation of the halo-artifact in ^{68}Ga-PSMA-11-PET/MRI. PLoS One 2017;12:e0183329.
[31] Szabo Z, Mena E, Rowe SP, et al. Initial evaluation of [^{18}F]DCFPyL for prostate-specific membrane antigen (PSMA)-targeted PET imaging of prostate cancer. Mol Imaging Biol 2015;17:565–74.
[32] Wurzer A, DiCarlo D, Schmidt A, et al. Radiohybrid ligands: a novel tracer concept exemplified by ^{18}F- or ^{68}Ga-labeled rhPSMA-inhibitors. J Nucl Med 2020;61:735–42.
[33] Foxton C, Grønlund RV, Simon J, et al. Preclinical evaluation of a novel radioligand therapy for patients with prostate cancer: biodistribution and efficacy of ^{177}Lu-rhPSMA-10.1 in comparison with ^{177}Lu-PSMA-I&T. J Nucl Med 2022;63(Suppl 2):2567.